Photochemical & Photobiological Sciences

PAPER

View Article Online
View Journal | View Issue

Cite this: *Photochem. Photobiol. Sci.*, 2016, **15**, 235

Fluorescence quenching in β-cyclodextrin vesicles: membrane confinement and host–guest interactions†

Frauke Schibilla,[a] Linda Stegemann,[b] Cristian A. Strassert,[b] Fabio Rizzo*[c] and Bart Jan Ravoo*[a]

Received 4th June 2015,
Accepted 23rd December 2015

DOI: 10.1039/c5pp00226e

www.rsc.org/pps

Fluorescent β-cyclodextrin vesicles (β-CDV) that display host cavities available for host–guest interactions at the vesicle surface were prepared by incorporation of the hydrophobic spirobifluorene-based dye **1** into the membrane of unilamellar vesicles. Fluorescence quenching of dye **1** was observed in the presence of different quenchers. Methyl viologen **2** does not quench dye **1** because it does not bind to β-CDV. 4-Nitrophenol **3** and 4-nitrophenol covalently connected to adamantane **4** quench the fluorescence of dye **1** in neutral solution, but by different mechanisms according to lifetime measurements. The quenching efficiency of **3** is pH dependent due to the presence of the phenolate form. Competition experiments with excess host and guest showed that **3** is likely to diffuse in and out of the membrane, while **4** forms an inclusion complex with β-CDV leading to close contact and efficient quenching. Our findings confirm that this dynamic supramolecular system is a versatile model to investigate quenching and recognition processes in bilayer membranes.

Introduction

Fluorescence quenching describes any process decreasing the intensity of the radiative decay of the emitting compounds. Quenching resulting from collisional encounter (dynamic quenching) and complex formation (static quenching) requires molecular contact between the quencher and the fluorophore and can thus be used to analyze the interaction between molecules.[1] Fluorescence quenching is often used to detect molecular recognition in sensors, which play an important role in biology as well as chemical analysis.[2] Among others, fluorescence quenching has applications in biochemistry such as the investigation of accessibility and localization of probes in a membrane or protein.[1,3] Furthermore, quenching is used for the detection of analytes in fluorescent chemosensors with high sensitivities and fast response times.[4–7] It is important to understand and control quenching processes in order to design and construct selective chemosensors.

Almost all biological processes depend on molecular recognition. Vesicles are widely used as models for biological membranes.[8,9] Vesicles can encapsulate water-soluble molecules in the aqueous interior and incorporate hydrophobic molecules into the bilayer membrane. Synthetic amphiphiles used to form vesicles can additionally include a binding motif which selectively binds complementary molecules. Vesicles are attractive systems to control photophysical processes such as quenching.[10,11] Photochemical reactivity is often enhanced by binding the quencher and the fluorophore to vesicles compared to homogeneous solutions.[12] For example, electron transfer from hydrophobic molecules incorporated into the membrane of liposomes to molecules bound electrostatically at the surface of the vesicle was investigated.[13,14] Other reports describe the preparation of an artificial photosynthetic reaction center incorporated into the bilayer of a liposome[15] and the improvement of the efficiency of electron transfer by using charged photosensitizers adsorbed on charged vesicles.[16] Also luminescent chemosensing vesicles have been described.[17–19]

Among the amphiphilic compounds used to form vesicles, modified cyclodextrins (CDs) appear very interesting as stimuli-responsive nanomaterials due to their host–guest properties.[20] In fact, CDs are able to act as a host for hydrophobic molecules in aqueous solution and for example are used as molecular encapsulators in pharmaceutical applications.[21–23] In addition, amphiphilic CDs form self-assembled nanostructures.[24] Vesicles consisting of β-CD amphiphiles (β-cyclo-

[a]*Organic Chemistry Institute and CeNTech, Westfälische Wilhelms-Universität Münster, Corrensstr. 40, D-48149 Münster, Germany. E-mail: b.j.ravoo@uni-muenster.de*
[b]*Physical Institute and CeNTech, Westfälische Wilhelms-Universität Münster, Heisenbergstr. 11, D-48149 Münster, Germany*
[c]*Istituto di Scienze e Tecnologie Molecolari (ISTM), CNR, Via Golgi 19, I-20133 Milano, Italy. E-mail: fabio.rizzo@istm.cnr.it*
†Electronic supplementary information (ESI) available. See DOI: 10.1039/c5pp00226e

dextrin vesicles, β-CDV) can encapsulate molecules in their aqueous interior, incorporate hydrophobic molecules into the membrane and form selective inclusion complexes at the surface of the vesicle.[25] For example, the incorporation of hydrophobic, magnetic nanoparticles into the membrane of β-CDV and directed assembly by magnetic forces and photoresponsive hydrophobic guest molecules have been reported.[26] Studies on the modification of host–guest interactions at β-CDV in the presence of competitive host or guest are also reported in the literature.[27,28] Förster resonance energy transfer (FRET) between a hydrophobic dye incorporated into the membrane of β-CDV acting as a donor and an acceptor fluorophore bearing adamantane, a well-known guest for β-CD, was used to investigate the dynamic multivalent molecular recognition of CDV.[29] Thus, β-CDV appears as a suitable system to control photophysical processes by the combination of hydrophobic co-partitioning and host–guest interactions. Recently, there have been a number of reports on the combination of chromophores with β-CDV or CD nanoparticles. The integration of photosensitizers in β-CDV or CD nanoparticles may potentially find application in nanomedicine as a system for photodynamic therapy.[21,30–32] However, systematic photophysical studies of these structures are rare.[33] In this paper we use the β-CDV as a model membrane to investigate the quenching of the fluorescence of an incorporated dye with guest compounds interacting in a different way with β-CDV. In particular, we describe the incorporation of spirobifluorene chromophore **1**[34] (2,7-bis-(4-(*N*,*N*-diphenylamino)phen-1-yl)-9,9-spirobifluorene) into the membrane of β-CDV and the investigation of fluorescence quenching by three different quenchers depicted in Chart 1.

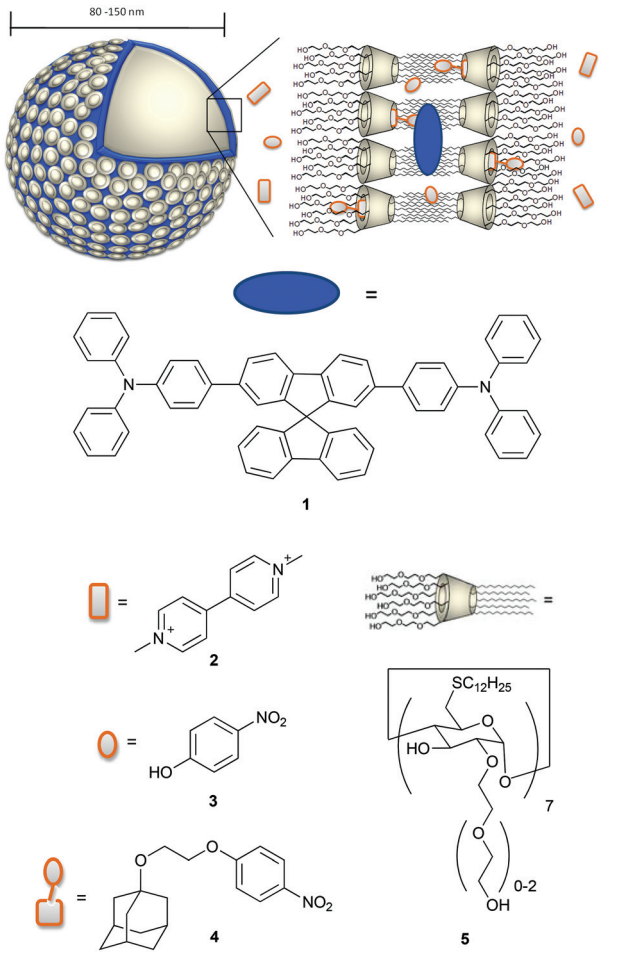

Chart 1 Schematic representation of β-CDV **5** with incorporated spirobifluorene-based dye **1** and different binding modes of quenchers methyl viologen **2**, 4-nitrophenol **3** and 4-nitrophenol covalently connected to adamantane **4**.

Methyl viologen **2** (commonly called paraquat) is widely used as a herbicide and it is highly toxic to humans and animals. People working with this herbicide are more likely to develop Parkinson's disease.[35,36] Also 4-nitrophenol **3** is toxic, hazardous for the environment and suspected to be carcinogenic. It is used as an important intermediate in industrial synthesis for explosives, pesticides and drugs and is eventually released to the environment as waste.[37] The detection of paraquat and 4-nitrophenol and their derivatives is discussed in the recent literature.[38–41] To increase the affinity of **3** to CD, we synthesized 4-(2-((adamant-1-yl)oxy)ethoxy)nitrobenzene **4** in which **3** is covalently connected to adamantane. The fluorescence quenching of **1** was investigated using fluorescence spectroscopy and lifetime measurements.

Results and discussion

Spirobifluorene derivative **1**[34] and amphiphilic β-CD **5**[25,42] were synthesized as described previously. Experimental details of the synthesis of **4** are reported in the ESI.† The highly hydrophobic spirobifluorene derivative **1** shows an intense luminescence in the blue region. Due to its rigid cross-like shape, π–π stacking and aggregation are hampered even at high concentrations. Thus, we can reasonably exclude that the emission is affected by side effects such as the formation of excimers.[34] Therefore, **1** is highly suitable as a photophysical membrane probe.

Unilamellar β-CDV with incorporated dye **1** were prepared by sonication and extrusion in phosphate buffer at pH 7.2. The average diameter of the vesicles was around 120 nm according to dynamic light scattering (DLS) measurements. The concentration of heptakis[6-deoxy-6-dodecylthio-2-oligo(ethyleneoxide)]-β-cyclodextrin (**5**) was 100 μM, while the average amount of incorporated dye **1** was around 6 μM calculated by absorption measurements (the dye's absorbance lies approximately between 0.40 and 0.45). It is important to note that this calculation is strongly affected by scattered light due to the presence of vesicles. Fig. 1 shows the absorption and emission spectra of **1** incorporated into β-CDV. The absorption spectrum shows the π–π* band with a maximum at 375 nm. The emission band has a peak at 420 nm for an excitation wavelength (λ_{ex}) of 375 nm, slightly blue shifted compared to the fluorescence in solution.[34]

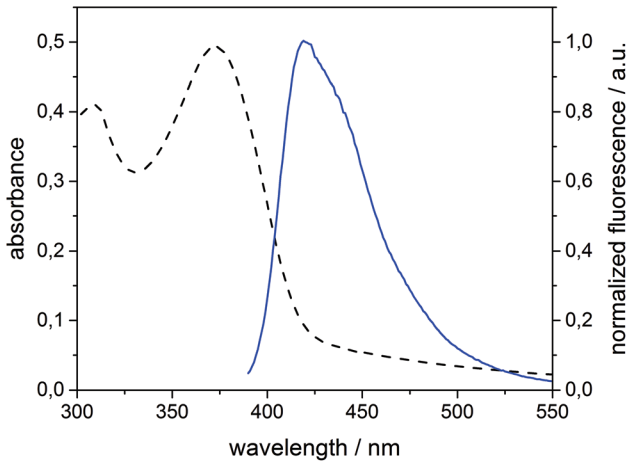

Fig. 1 Absorption (dashed line) and normalized fluorescence intensity (solid line) spectra (λ_{exc} = 375 nm) of **1** (6 μM) incorporated into β-CDV in phosphate buffer (pH 7.2).

To study the distribution of the dye in the membrane microscopically, giant unilamellar vesicles (GUVs) with incorporated **1** were prepared by electroformation. Microscopy images of these GUVs (Fig. 2) indicate spherical and elongated vesicles with slightly irregular surfaces. Similar GUVs were previously described by our group for pure β-CDV.[43] GUVs show fluorescence exclusively in the region of the membrane and thus these observations confirm that dye **1** is confined to the membrane.

Although the dye and the cyclodextrin are in close proximity, we can reasonably exclude the formation of inclusion complexes. In fact, the rigid spirobifluorene derivative **1** appears too large to bind the cavity of β-CD and the peripheral phenyl rings show low binding constant values.[44,45] Thus all cavities along the vesicle can be considered available for host–guest interactions. The vesicles are stable for more than one day and their stability is not affected by the addition of quenchers **2**, **3** or **4** up to 100 μM.

Compounds **2**–**4** all quench the fluorescence of **1** in organic solutions, but each has a different affinity for β-CD. Dicationic quencher **2** is highly hydrophilic and thus is not able to form host–guest complexes with β-CD. Quencher **3** is soluble in water, but shows moderate affinity towards β-CD ($K_a \approx 10^2$–10^3 M^{-1}),[46] while the adamantane derivative **4** strongly binds β-CD[47] ($K_a \approx 10^4$ M^{-1}) and is not soluble in water. On the basis of these data, we assumed a dynamic partitioning of nitrophenol **3** between the solution and β-CDV and a preferential localization of **4** at the surface of β-CDV close to the dye. To investigate the fluorescence quenching, emission spectra of **1** incorporated into β-CDV were measured in the presence of **2**–**4** at different concentrations (see ESI Fig. S1 and S2†). The concentration dependent quenching of **1** by **2**–**4** shown in Fig. 3 is reported as the ratio F/F_0 at the emission maximum (420 nm), where F and F_0 are the emission intensities of **1** incorporated into β-CDV in the presence and absence of quenchers, respectively. This ratio allows a direct comparison of the quenching efficiency among different quenchers. The fluorescence data F and F_0 were corrected using the formula reported in the ESI,† which takes into account the co-absorption of **1** and the quencher at the excitation wavelength (absorption at λ_{exc} = 375 nm) and the inner filter effect at the emission wavelength (absorption at λ_{em} = 420 nm) (see ESI Fig. S3†).[1] We emphasize the importance of the correction factor, since in fact the *uncorrected* data would suggest that **3** and **4** have the same

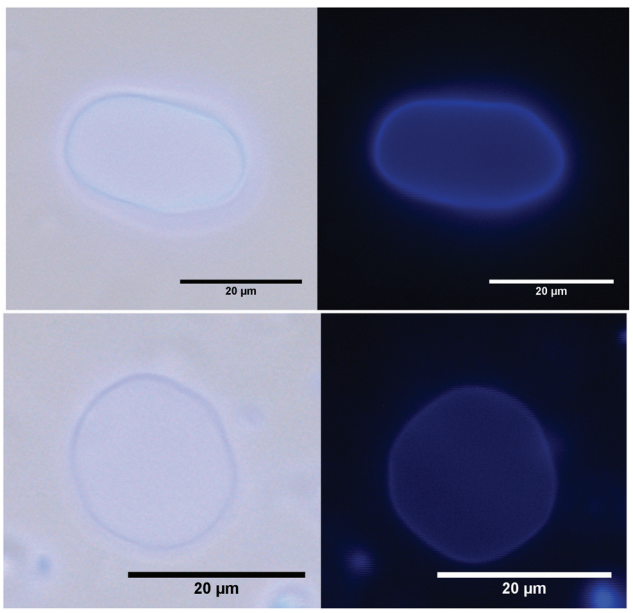

Fig. 2 Microscopy images of GUVs with incorporated **1**: left: light microscopy with UV-irradiation. Right: fluorescence microscopy.

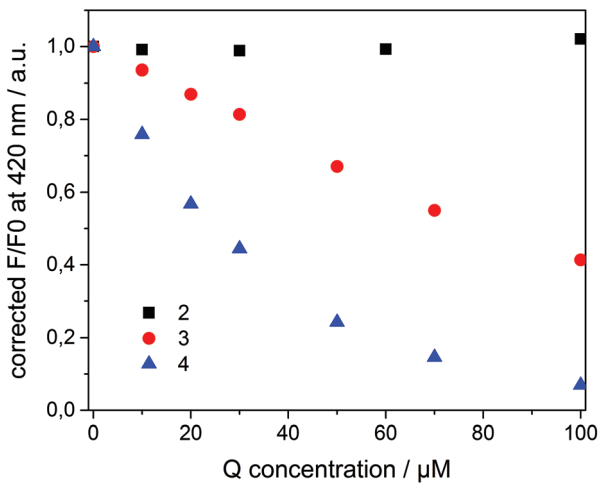

Fig. 3 F/F_0 at 420 nm (λ_{exc} = 375 nm) of **1** incorporated into β-CDV in phosphate buffer (pH 7.2) as a function of the concentration of the quencher (Q) **2**, **3** and **4**. F and F_0 are the emission maxima in the presence and absence of quenchers, respectively.

quenching efficiency (see ESI Fig. S4†). In the text, we refer to the *corrected* values of F and F_0.

As depicted in Fig. 3, the presence of **2** does not influence the fluorescence in vesicle solution (black squares). As expected, the dicationic and hydrophilic methyl viologen remains in solution resulting in a large distance between **1** and **2**, while close contact is necessary for quenching. In contrast, **3** (red circle) and **4** (blue triangle) quench the fluorescence of the dye. Despite their similar structure, **4** results to be more efficient than **3**.

To investigate the quenching process in more detail the Stern–Volmer plot was used. The classical Stern–Volmer equation can be written as $F_0/F = 1 + K_{SV}[Q]$, where F_0 and F is the intensity of the fluorophore in the absence and presence of the quencher, K_{SV} is the Stern–Volmer constant and [Q] is the concentration of the quencher. The equation shows linear behavior and describes dynamic ($\tau_0/\tau = F_0/F$) or static ($\tau_0/\tau = 1$) quenching (τ_0 and τ are the lifetime of the dye in the absence and in the presence of quencher Q, respectively). In some cases dynamic and static quenching appear simultaneously resulting in a positive deviation from linearity. Therefore, the adjusted Stern–Volmer plot, $F_0/F = (1 + K_D[Q])(1 + K_s[Q])$, can be divided into a linear dynamic (K_D) and linear static (K_S) part, whereby the dynamic part ($1 + K_D[Q]$) is equal to τ_0/τ.[1]

To analyze the Stern–Volmer plot, the fluorescence lifetime of **1** incorporated into β-CDV was measured as a function of the concentration of **2**, **3** or **4** (Fig. 4). The average lifetime (τ_0) of dye **1** incorporated into β-CDV in aqueous solution is 1.0 ns, which is slightly lower than the value reported for **1** in organic solvent (1.3 ns).[34] Upon increasing the concentration of **2** in solution, the lifetime remains almost constant. The addition of **3** leads to a lower decrease in lifetime (τ (100 μM **3**) = 0.86 ns) compared to the addition of **4** (τ (100 μM **4**) = 0.45 ns) (Fig. 4). The different behaviours of **3** and **4** indicate the operation of dissimilar quenching mechanisms. The Stern–Volmer plots for quenching of **1** incorporated into β-CDV with **3** and **4** are shown in Fig. 5. As depicted in Fig. 5, the slope of F_0/F in the presence of **3** or **4** shows a positive deviation from linearity, which refers to a complex quenching process compared to the classic behaviour.

In order to interpret these data, the dynamic and static contributions of the quenching have to be evaluated separately. The dynamic part of the quenching can be determined by lifetime measurements and showed linear behaviour, as indicated in the following equation:

$$\frac{\tau_0}{\tau} = 1 + K_D[Q]$$

The dynamic Stern–Volmer constant K_D was calculated to be 1.75×10^3 M^{-1} for **3** and 1.2×10^4 M^{-1} for **4**. In both cases the contribution of dynamic quenching to the decrease of luminescence is high. The second quenching contribution

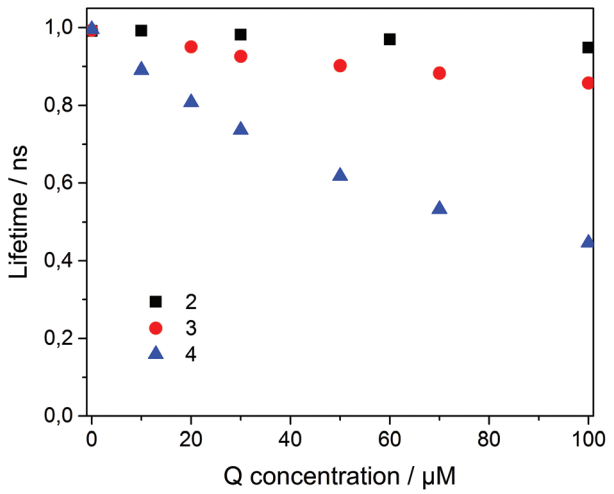

Fig. 4 Fluorescence lifetime (λ_{exc} = 375 nm) of **1** incorporated into β-CDV in phosphate buffer (pH 7.2) dependent on the concentration of the quencher (Q) **2** (black square), **3** (red circle) and **4** (blue triangle).

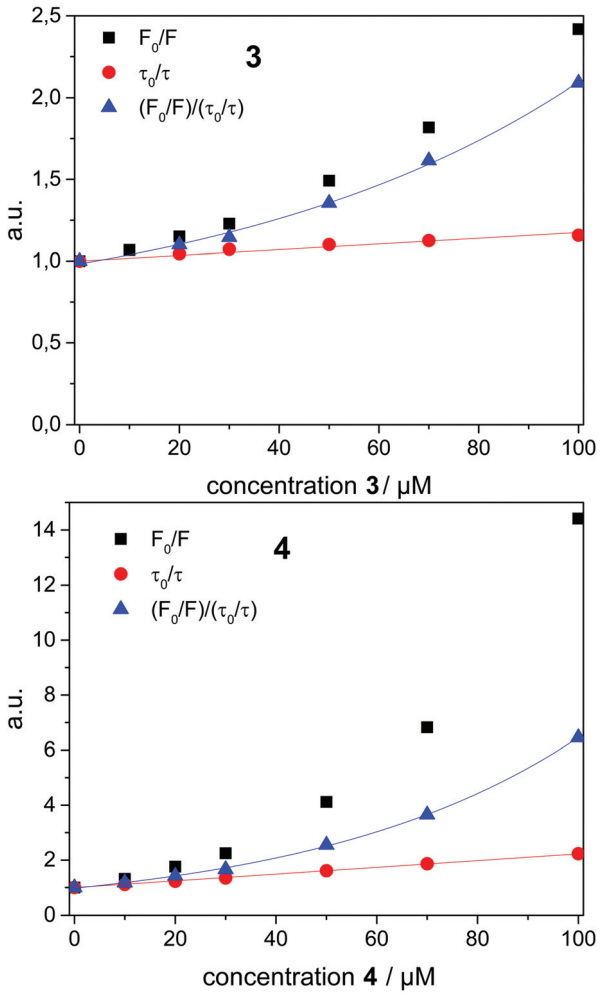

Fig. 5 Stern–Volmer plot (F_0/F, black square) divided into dynamic (τ_0/τ, red circle) and apparent static quenching ($(F_0/F)/(\tau_0/\tau)$, blue triangle) for quenching of **1** incorporated into β-CDV at pH 7.2 dependent on different concentrations of **3** (up) and **4** (down).

$((F_0/F)/(\tau_0/\tau))$ could be assigned to apparent static quenching, but shows an exponential growth instead of linear behaviour (blue triangle in Fig. 5). The upward curvature cannot be attributed to classic static quenching with the formation of a ground-state non-fluorescent complex, but to the existence of a sphere of effective quenching, as predicted by the Perrin's model.[48] In fact, the fluorophore is strictly confined in the membrane with low diffusion freedom. As a consequence, the quencher can act only when it is located near the dye at the moment of excitation. Because of the high local concentration in the vesicle, the positive deviation from linearity in the Stern–Volmer plot with exponential behaviour can be associated with a simultaneous dynamic and static quenching in which the sphere of quenching has to be considered. The equation of the sphere of quenching is $F_0/F = (1 + K_D[Q]) \times e^{VN_A[Q]}$ where V is the volume of the sphere and N_A the Avogadro's number.[1] By plotting $\ln\left(\frac{F_0/F}{1+K_D}\right)$ *vs.* [Q] it is possible to calculate the radius of the quenching sphere. We obtained a value for R of 15 Å and 19 Å for **3** and **4** respectively, which are in agreement with the thickness of the membrane (42 Å).[25]

Additionally, the quantum yield (QY) was measured to calculate the rates of radiative and nonradiative decay (k_r and k_{nr}).

$$k_r = \frac{QY}{\tau}, \quad k_{nr} = \frac{(1-QY)}{\tau}$$

The QY of the spiro-compound incorporated into β-CDV without the quencher is 45% and thus lower than for **1** in DMF (87%).[34] The QY decreases with increasing concentration of **3** or **4**, whereby the absorbance of quenchers **3** and **4** overlaps the absorbance of **1** and thus the measured quantum yield had to be corrected (see ESI Fig. S3†).

In the absence of the quencher, the rate of radiative decay of **1** incorporated into β-CDV in buffer solution (4.5×10^8 s^{-1}) is smaller than in DMF (6.8×10^8 s^{-1}), while the rate of nonradiative decay is much higher (β-CDV solution: 5.5×10^8 s^{-1}, DMF: 1.0×10^8 s^{-1}).[34] Although the formation of excimers can be excluded, the incorporation into the membrane influences the emission of **1**. However, because k_{nr} is strictly connected to the quenching process, we focused our attention on its variations by increasing the concentration of quenchers in buffer solution (Table 1). By adding different amounts of quencher **3** or **4**, an increase in the rate of nonradiative decay was measured. The increase is much higher for **4** than for **3**, which strengthens the interpretation of different quenching mechanisms involved. The high increase of k_{nr} for **4** can be explained by taking into account the high affinity of **4** to the cavity of β-CDV.

Table 1 Rates of nonradiative decay (k_{nr}) for **1** incorporated into β-CDV in phosphate buffer (pH 7.2) with different concentrations of **3** and **4**

μM	k_{nr}(**3**) [10^8 s^{-1}]	k_{nr}(**4**) [10^8 s^{-1}]
0	5.5	
50	9.6	14.6
100	10.8	21.8

Due to the host–guest interaction between the cyclodextrin cavity and adamantane, almost all quencher molecules are located in the proximity of the membrane, which leads to a high local concentration of **4** close to the dye. We can then conclude that k_{nr} data are in agreement with the sphere of quenching interpretation.

In the case of **3**, the distribution of the quencher in the proximity of **1** appears very different for **4**. The 4-nitrophenol has low affinity for the hydrophobic cavity of β-CD ($K_a \approx 10^2$–10^3 M^{-1}).[46] However, it might also be able to diffuse through the hydrophobic membrane of the vesicles due to its aromatic and apolar structure. Thus, **3** can come in close contact to **1** and quench its fluorescence. On the other hand, **3** is soluble in water, which probably leads to a partitioning of **3** between the vesicles and aqueous solution.

To interpret the quenching behaviour of **3**, also the pH has to be considered. In phosphate buffer at pH = 7.2, 4-nitrophenol (pK_a = 7.15)[49] exists in its protonated (phenol) and deprotonated (phenolate) form, while more than 99.9% of **3** is protonated in acetate buffer at pH = 4.5 and deprotonated in carbonate buffer at pH = 10.3, respectively. To investigate the effect of pH, β-CDV with incorporated dye **1** were additionally prepared in acetate buffer and carbonate buffer. Absorption and emission spectra were recorded at different concentrations of **3**. In Fig. 6 the normalized fluorescence intensity of **1** in β-CDV is reported at various concentrations of 4-nitrophenol at different pH values. The general trend seems to indicate that the quenching is more efficient if **3** is deprotonated (phenolate) than if it is protonated (phenol), even though the association constant of 4-nitrophenol and 4-nitrophenolate with β-CD is approximately the same.[47] This effect can be explained by considering the absorption spectra of 4-nitrophenol as a function of pH (see ESI Fig. S5†).

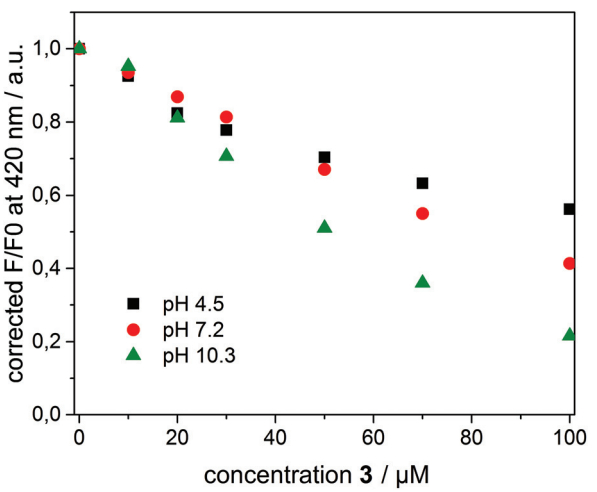

Fig. 6 F/F_0 at 420 nm (λ_{exc} = 375 nm) of **1** incorporated into β-CDV as a function of the concentration of **3** at pH 4.5 (black square), 7.2 (red circle) and 10.3 (green triangle). F and F_0 are the emission maxima in the presence and absence of quenchers, respectively.

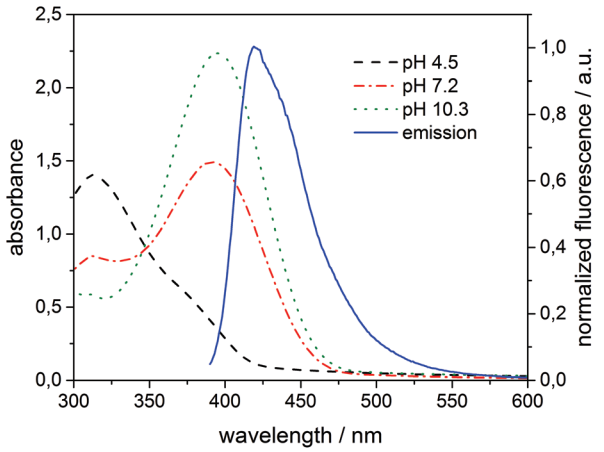

Fig. 7 Absorption of **3** (100 μM) added to **1** (6 μM) incorporated into β-CDV at different pH values and normalized fluorescence intensity (λ_{exc} = 375 nm) of the system **1**/β-CDV without quenchers.

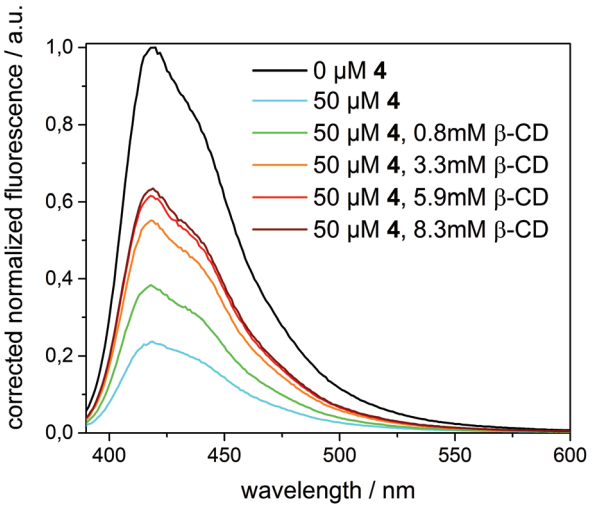

Fig. 8 Fluorescence intensity (λ_{exc} = 375 nm) of **1** (6 μM) incorporated into β-CDV in phosphate buffer (pH 7.2) before and after the addition of **4** (50 μM) and different amounts of β-CD (0–8.3 mM). The spectra are normalized by dividing the data by the intensity of **1** at 420 nm in the absence of quenchers.

The absorption maximum of **3** is at 310 nm in acid solution (phenol) and at 405 nm in basic solution (phenolate), while the emission peak of **1** is at 420 nm (Fig. 7). Thus, the variation of pH results in a more extended overlap between the emission of **1** and the absorption of **3** and in an increasing of the inner filter effect. Although the data were corrected by a factor which takes into account the co-absorption and the reabsorption of the emitted light, at pH 7.2 and 10.3 the high absorption band of **3** at higher concentrations can give an overestimation of the quenching. In fact, as reported in the literature[48,50] the correction factors regarding the inner filter effect are affected by uncertainties difficult to estimate.

However, an alternative explanation in agreement with the recorded data can be also given. The charged phenolate can interact with **1** leading to the formation of a non-emitting ground-state complex (static quenching). This hypothesis is justified by examining the Stern–Volmer plot at different pH values (see ESI Fig. S6†). F_0/F appears linear at pH 4.5 suggesting a pure dynamic quenching contribution, while at pH 7.2 and 10.3 the plot leads to an exponential fit. The increased upwards curvature can be associated with an additional static quenching contribution described by the above-mentioned sphere of quenching model.

Finally, the quenching effect of **3** and **4** was also analyzed by the addition of a competitive, nonquenching host (β-CD) and guest (1-adamantane methanol) to obtain more information about host–guest interactions involved in the supramolecular system. In the case of quencher **3**, the addition of an excess of β-CD (up to 8 mM) or 1-adamantane methanol (50 μM) to **1** in β-CDV quenched by **3** (50 μM) does not influence the fluorescence intensity. This strengthens the interpretation that **3** is not bound to the CD, but diffuses through the hydrophobic membrane. Thus, the quenching action exerted by **3** can be definitely attributed to its partitioning and diffusion between the aqueous phase and the membrane and not by host–guest interaction.

A completely different behaviour was observed in the case of quencher **4**, as depicted in Fig. 8. Upon addition of an excess of β-CD (up to 8.3 mM) to **1** in β-CDV quenched by **4** (50 μM), the fluorescence intensity increased, even though the initial intensity of **1** in the absence of the quencher cannot be fully restored. (A higher concentration of β-CD cannot be achieved due to its limited solubility.) Thus, we can reasonably suppose that β-CD in solution binds competitively to **4** decreasing the amount of the quencher in β-CDV. The lower concentration of **4** in proximity to **1** results in less efficient quenching.

In contrast, the addition of a competitive guest (3.5 mM of 4-diamantane carboxylic acid, 10 mM of 1-adamantane carboxylic acid or 50 μM of 1-adamantane methanol) after quenching with **4** (50 μM) induces a further decrease of the fluorescence intensity. This effect could be explained with a partial displacement of **4** from the β-CD cavities by the presence of the competitive guest. Due to its hydrophobic character, the nitrophenolate-adamantane derivative diffuses into the membrane leading to a higher effective concentration of the quencher in close proximity to the dye. This strengthens the interpretation that the effective quenching of **4** is due to host–guest interactions.

Conclusion

Hydrophobic spirobifluorene **1** was incorporated into the membrane of β-CDV and its photophysical properties in the presence of quenchers have been investigated. Hydrophilic and dicationic methyl viologen (paraquat) **2** does not interact with the vesicles and thus does not quench the fluorescence of **1**. 4-Nitrophenol **3** and 4-nitrophenolate covalently linked to

adamantane **4** quench the fluorescence of **1** through different mechanisms due to their dissimilar affinity to the cavity of β-CD. For both compounds the Stern–Volmer analysis reveals the presence of a dynamic and an apparent static quenching component, which can be explained within the sphere of effective quenching model. Quencher **3** is partitioned between the membrane and the aqueous phase because of its solubility in water and its low affinity for β-CD, whereas **4** is confined in the vesicle membrane leading to a higher quenching efficiency. The quenching behaviour of 4-nitrophenol (**3**) is pH dependent and appears more efficient under basic conditions. Competitive host or guest does not influence the emission intensity in the case of **3**, confirming the hypothesis that the quenching is not controlled by host–guest interactions. In contrast, **4** strongly quenches the fluorescence due to host–guest interactions owing to the high affinity between the adamantane and cyclodextrin cavities. Competitive host decreases the quenching, while competitive guest increase the quenching effect. In general, we can conclude that quenching can be controlled by hydrophobic and host–guest interactions between the quencher and vesicle. The investigated supramolecular system appears as a versatile model to study quenching processes and molecular recognition at membrane surfaces. Future applications in the field of chemosensors can be foreseen.

Experimental section

Vesicle preparation

A 1.0 mM solution of **5** and a 0.1 mM solution of **1** were prepared in chloroform. 500 μL of both solutions were added to a round bottom flask. The solvent was removed by a stream of argon to yield a thin film. The solvent was completely removed under high vacuum for 5 min. Buffer solution (20 mM, 5 mL) was added and stirred overnight. The resulting suspension was sonicated for 15 min. Afterwards the suspension was extruded with a LiposoFast manual extruder (AVESTIN Europe GmbH, Mannheim, Germany) by repeatedly passing it through a polycarbonate membrane. The size (between 80 and 150 nm) was confirmed by DLS measurements which is relative to an approximate vesicle concentration between 0.2 and 0.8 nM.[25]

For the preparation of giant unilamellar vesicles (GUVs) 0.50 mM **5** and 0.05 mM **1** were dissolved in chloroform. Two electrode slices coated with ITO were covered with a thin layer of the solution (22.5 μL). The solvent was evaporated in a vacuum oven at 50 °C. After adding buffer solution (1 mM HEPES, 300 mM sucrose, pH 7.2), an alternating electric field was applied (1 V, 10 Hz) at 50 °C for 1 h. The solution was spread on a microscope slide coated with bovine serum albumin to reduce surface adsorption and investigated by light and fluorescence microscopy.

Dynamic light scattering (DLS)

DLS measurements were performed on a Nano ZS Zetasizer (Malvern Instruments Ltd, Worcestershire, UK) with disposable semi-micro PMMA cuvettes (BRAND GmbH & Co. KG, Wertheim, Germany) with a path length of 1 cm at 25 °C. The control of the spectrometer and data analysis was performed with the software Zetasizer 6.32 (JASCO Malvern Instruments Ltd, Worcestershire, UK). The average size of the vesicles was measured before and after addition of the quencher.

Microscopy

Light and fluorescence microscopy was performed by a Leica DMRE with a TCS SL scanning unit (Leica Microsystems Heidelberg GmbH, Mannheim, Germany).

Photophysical characterization

Absorption spectra were measured on a Varian Cary 5000 double-beam UV-Vis-NIR spectrometer (Agilent Technologies, Santa Clara, USA) and were baseline corrected. Steady-state emission spectra and lifetimes were recorded on a FluoTime300 spectrometer (PicoQuant, Berlin, Germany) equipped with a 300 W ozone-free Xe lamp (250–900 nm), a 10 W Xe flash-lamp (250–900 nm, pulse width <10 μs) with repetition rates of 0.1–300 Hz, an excitation monochromator (Czerny–Turner 2.7 nm mm^{-1} dispersion, 1200 grooves per mm, blazed at 300 nm), diode lasers (pulse width <80 ps) operated by a computer-controlled laser driver PDL-820 (repetition rate up to 80 MHz, burst mode for slow and weak decays), two emission monochromators (Czerny–Turner, selectable gratings blazed at 500 nm with 2.7 nm mm^{-1} dispersion and 1200 grooves per mm, or blazed at 1250 nm with 5.4 nm mm^{-1} dispersion and 600 grooves per mm), Glan–Thompson polarizers for excitation (Xe-lamps) and emission, a Peltier-thermostatized sample holder (Quantum Northwest, Liberty Lake, USA) (−40 °C–105 °C), and two detectors, namely a PMA hybrid 40 (transit time spread FWHM <120 ps, 300–720 nm) and a R5509-42 NIR-photomultiplier tube (transit time spread FWHM 1.5 ns, 300–1400 nm) with external cooling (−80 °C) (Hamamatsu Photonics, Ltd, Shizuoka, Japan). Steady-state and fluorescence lifetimes were recorded in TCSPC mode by a PicoHarp 300 (minimum base resolution 4 ps). Emission spectra were corrected for source intensity (lamp and grating) by standard correction curves. Lifetime analysis was performed using the commercial FluoFit software. The quality of the fit was assessed by minimizing the reduced chi squared function (χ^2) and visual inspection of the weighted residuals and their autocorrelation. Luminescence quantum yields were measured with an absolute PL quantum yield measurement system (C9920-02) (Hamamatsu Photonics, Ltd, Shizuoka, Japan) equipped with a L9799-01 CW Xenon light source (150 W), monochromator, C7473 photonic multi-channel analyzer, integrating sphere and employing U6039-05 PLQY measurement software (Hamamatsu Photonics, Ltd, Shizuoka, Japan).

NMR

NMR-spectra were recorded on a Bruker AV 300 (Bruker Corporation, Billerica, Massachusetts, USA). The measurements were performed in deuterated solvents at room temperature. MestReNova 9.0 (Mestrelab Research S. L., Santiago de Com-

postela, Spain) was used for data analysis. The chemical shifts are given in parts per million (ppm) relative to the residual solvent signals. The multiplicity of the signals is labeled as singlet (s), doublet (d), triplet (t), quartet (q), heptet (h), multiplet (m) and broad (br) and the coupling constant J is noted in Hz.

Mass spectrometry

Electrospray ionization (ESI) mass spectra were recorded on a MicroTof (Bruker Daltonics, Bremen, Germany), while MALDI mass spectra were measured on a Autoflex Speed (Bruker Daltonics, Bremen, Germany).

Infrared-spectroscopy (IR)

IR Spectra were recorded on a Varian Fourier transformation IR spectrometer Type 310 (Agilent Technologies, Santa Clara, USA) with potassium bromide pellets (KBr). The data was analyzed using the Resolution Pro software (Agilent Technologies, Santa Clara, USA) and all spectral data were corrected by subtracting the background signal.

Acknowledgements

F. R. thanks the Deutscher Akademischer Austauschdienst (DAAD) for the fellowship. This work was supported by the Deutsche Forschungsgemeinschaft (DFG TRR 61).

References

1 J. R. Lakowicz, *Principles of fluorescence spectroscopy*, Springer, New York, 3rd edn, 2006.
2 A. P. de Silva, H. Q. N. Gunaratne, T. Gunnlaugsson, A. J. M. Huxley, C. P. McCoy, J. T. Rademacher and T. E. Rice, Signaling recognition events with fluorescent sensors and switches, *Chem. Rev.*, 1997, **97**, 1515–1566.
3 G. A. Caputo and E. London, Using a novel dual fluorescence quenching assay for measurement of tryptophan depth within lipid Bilayers to determine hydrophobic alpha-helix locations within membranes, *Biochemistry*, 2003, **42**, 3265–3274.
4 F. Mancin, E. Rampazzo, P. Tecilla and U. Tonellato, Self-assembled fluorescent chemosensors, *Chem. – Eur. J.*, 2006, **12**, 1844–1854.
5 G. Ghale and W. M. Nau, Dynamically Analyte-Responsive Macrocyclic Host-Fluorophore Systems, *Acc. Chem. Res.*, 2014, **47**, 2150–2159.
6 T. Pradhan, H. S. Jung, J. H. Jang, T. W. Kim, C. Kang and J. S. Kim, Chemical sensing of neurotransmitters, *Chem. Soc. Rev.*, 2014, **43**, 4684–4713.
7 R. Martinez-Manez and F. Sancenon, Fluorogenic and chromogenic chemosensors and reagents for anions, *Chem. Rev.*, 2003, **103**, 4419–4476.
8 J. Voskuhl and B. J. Ravoo, Molecular recognition of bilayer vesicles, *Chem. Soc. Rev.*, 2009, **38**, 495–505.
9 H. Valkenier, N. Lopez Mora, A. Kros and A. P. Davis, Visualization and quantification of transmembrane ion transport into giant unilamellar vesicles, *Angew. Chem., Int. Ed.*, 2015, **54**, 2137–2141.
10 B. Gruber and B. König, Self-assembled vesicles with functionalized membranes, *Chem. – Eur. J.*, 2013, **19**, 438–448.
11 M. A. Fox and M. Chanon, *Photoinduced electron transfer, Part B*, Elsevier, Amsterdam, 1988.
12 B. Armitage and D. F. O'Brien, Lipid Bilayer Enhanced Photoinduced Electron-Transfer, *J. Am. Chem. Soc.*, 1991, **113**, 9678–9679.
13 B. Armitage and D. F. O'Brien, Vectorial Photoinduced Electron-Transfer between Phospholipid Membrane-Bound Donors and Acceptors, *J. Am. Chem. Soc.*, 1992, **114**, 7396–7403.
14 P. J. Clapp, B. Armitage, P. Roosa and D. F. O'Brien, Efficient Photoinduced Orthogonal Energy and Electron-Transfer Reactions Via Phospholipid Membrane-Bound Donors and Accepters, *J. Am. Chem. Soc.*, 1994, **116**, 9166–9173.
15 G. Steinberg-Yfrach, P. A. Liddell, S. C. Hung, A. L. Moore, D. Gust and T. A. Moore, Conversion of light energy to proton potential in liposomes by artificial photosynthetic reaction centres, *Nature*, 1997, **385**, 239–241.
16 B. Limburg, G. Laisne, E. Bouwman and S. Bonnet, Enhanced Photoinduced Electron Transfer at the Surface of Charged Lipid Bilayers, *Chem. – Eur. J.*, 2014, **20**, 8965–8972.
17 S. Banerjee and B. König, Molecular Imprinting of Luminescent Vesicles, *J. Am. Chem. Soc.*, 2013, **135**, 2967–2970.
18 S. Banerjee, M. Bhuyan and B. König, Tb(III) functionalized vesicles for phosphate sensing: membrane fluidity controls the sensitivity, *Chem. Commun.*, 2013, **49**, 5681–5683.
19 A. Müller and B. König, Preparation of luminescent chemosensors by post-functionalization of vesicle surfaces, *Org. Biomol. Chem.*, 2015, **13**, 1690–1699.
20 A. P. Blum, J. K. Kammeyer, A. M. Rush, C. E. Callmann, M. E. Hahn and N. C. Gianneschi, Stimuli-Responsive Nanomaterials for Biomedical Applications, *J. Am. Chem. Soc.*, 2015, **137**, 2140–2154.
21 X. Ma and Y. L. Zhao, Biomedical Applications of Supramolecular Systems Based on Host-Guest Interactions, *Chem. Rev.*, 2015, **115**, 7794–7839.
22 Y. Kang, K. Guo, B. J. Li and S. Zhang, Nanoassemblies driven by cyclodextrin-based inclusion complexation, *Chem. Commun.*, 2014, **50**, 11083–11092.
23 E. M. M. Del Valle, Cyclodextrins and their uses: a review, *Process Biochem.*, 2004, **39**, 1033–1046.
24 F. Sallas and R. Darcy, Amphiphilic cyclodextrins - Advances in synthesis and supramolecular chemistry, *Eur. J. Org. Chem.*, 2008, 957–969.
25 P. Falvey, C. W. Lim, R. Darcy, T. Revermann, U. Karst, M. Giesbers, A. T. M. Marcelis, A. Lazar, A. W. Coleman, D. N. Reinhoudt and B. J. Ravoo, Bilayer vesicles of amphiphilic cyclodextrins: Host membranes that recognize guest molecules, *Chem. – Eur. J.*, 2005, **11**, 1171–1180.

26 J. H. Schenkel, A. Samanta and B. J. Ravoo, Self-Assembly of Soft Hybrid Materials Directed by Light and a Magnetic Field, *Adv. Mater.*, 2014, **26**, 1076–1080.
27 S. K. M. Nalluri, J. B. Bultema, E. J. Boekema and B. J. Ravoo, Photoresponsive Molecular Recognition and Adhesion of Vesicles in a Competitive Ternary Supramolecular System, *Chem. – Eur. J.*, 2011, **17**, 10297–10303.
28 N. Nayak and K. R. Gopidas, Unusual self-assembly of a hydrophilic β-cyclodextrin inclusion complex into vesicles capable of drug encapsulation and release, *J. Mater. Chem. B*, 2015, **3**, 3425–3428.
29 C. W. Lim, B. J. Ravoo and D. N. Reinhoudt, Dynamic multivalent recognition of cyclodextrin vesicles, *Chem. Commun.*, 2005, 5627–5629.
30 M. Trapani, A. Romeo, T. Parisi, M. T. Sciortino, S. Patane, V. Villari and A. Mazzaglia, Supramolecular hybrid assemblies based on gold nanoparticles, amphiphilic cyclodextrin and porphyrins with combined phototherapeutic action, *RSC Adv.*, 2013, **3**, 5607–5614.
31 C. Conte, A. Scala, G. Siracusano, N. Leone, S. Patane, F. Ungaro, A. Miro, M. T. Sciortino, F. Quaglia and A. Mazzaglia, Nanoassembly of an amphiphilic cyclodextrin and Zn(II)-phthalocyanine with the potential for photodynamic therapy of cancer, *RSC Adv.*, 2014, **4**, 43903–43911.
32 J. Voskuhl, U. Kauscher, M. Gruener, H. Frisch, B. Wibbeling, C. A. Strassert and B. J. Ravoo, A soft supramolecular carrier with enhanced singlet oxygen photosensitizing properties, *Soft Matter*, 2013, **9**, 2453–2457.
33 N. Kandoth, E. Vittorino, M. T. Sciortino, T. Parisi, I. Colao, A. Mazzaglia and S. Sortino, A Cyclodextrin-Based Nanoassembly with Bimodal Photodynamic Action, *Chem. – Eur. J.*, 2012, **18**, 1684–1690.
34 F. Polo, F. Rizzo, M. Veiga-Gutierrez, L. De Cola and S. Quici, Efficient Greenish Blue Electrochemiluminescence from Fluorene and Spirobifluorene Derivatives, *J. Am. Chem. Soc.*, 2012, **134**, 15402–15409.
35 F. Kamel, Epidemiology. Paths from pesticides to Parkinson's, *Science*, 2013, **341**, 722–723.
36 C. M. Tanner, F. Kamel, G. W. Ross, J. A. Hoppin, S. M. Goldman, M. Korell, C. Marras, G. S. Bhudhikanok, M. Kasten, A. R. Chade, K. Comyns, M. B. Richards, C. Meng, B. Priestley, H. H. Fernandez, F. Cambi, D. M. Umbach, A. Blair, D. P. Sandler and J. W. Langston, Rotenone, Paraquat, and Parkinson's Disease, *Environ. Health Perspect.*, 2011, **119**, 866–872.
37 C. Nistor, A. Oubina, M. P. Marco, D. Barcelo and J. Emneus, Competitive flow immunoassay with fluorescence detection for determination of 4-nitrophenol, *Anal. Chim. Acta*, 2001, **426**, 185–195.
38 R. Gao, N. Choi, S. I. Chang, S. H. Kang, J. M. Song, S. I. Cho, D. W. Lim and J. Choo, Highly sensitive trace analysis of paraquat using a surface-enhanced Raman scattering microdroplet sensor, *Anal. Chim. Acta*, 2010, **681**, 87–91.
39 H. Fang, X. Zhang, S. J. Zhang, L. Liu, Y. M. Zhao and H. J. Xu, Ultrasensitive and quantitative detection of paraquat on fruits skins via surface-enhanced Raman spectroscopy, *Sens. Actuators, B*, 2015, **213**, 452–456.
40 Z. N. Liu, J. G. Du, C. C. Qiu, L. H. Huang, H. Y. Ma, D. Z. Shen and Y. Ding, Electrochemical sensor for detection of p-nitrophenol based on nanoporous gold, *Electrochem. Commun.*, 2009, **11**, 1365–1368.
41 J. H. Ko, J. H. Moon, N. Kang, J. H. Park, H.-W. Shin, N. Park, S. Kang, S. M. Lee, H. J. Kim, T. K. Ahn, J. Y. Lee and S. U. Son, Engineering of Sn-porphyrin networks on the silica surface: sensing of nitrophenols in water, *Chem. Commun.*, 2015, **51**, 8781–8784.
42 F. Guillo, B. Hamelin, L. Jullien, J. Canceill, J. M. Lehn, L. Derobertis and H. Driguez, Synthesis of Symmetrical Cyclodextrin Derivatives Bearing Multiple Charges, *Bull. Soc. Chim. Fr.*, 1995, **132**, 857–866.
43 U. Kauscher, M. C. A. Stuart, P. Drucker, H. J. Galla and B. J. Ravoo, Incorporation of Amphiphilic Cyclodextrins into Liposomes as Artificial Receptor Units, *Langmuir*, 2013, **29**, 7377–7383.
44 I. Gomezorellana and D. Hallen, The Thermodynamics of the Binding of Benzene to Beta-Cyclodextrin in Aqueous-Solution, *Thermochim. Acta*, 1993, **221**, 183–193.
45 E. Siimer, M. Kobu and M. Kurvits, Thermochemical Study of Cyclodextrin Inclusion Complexes, *Thermochim. Acta*, 1990, **170**, 89–95.
46 G. L. Bertrand, J. R. Faulkner, S. M. Han and D. W. Armstrong, Substituent Effects on the Binding of Phenols to Cyclodextrins in Aqueous-Solution, *J. Phys. Chem.*, 1989, **93**, 6863–6867.
47 M. V. Rekharsky and Y. Inoue, Complexation thermodynamics of cyclodextrins, *Chem. Rev.*, 1998, **98**, 1875–1917.
48 B. Valeur, *Molecular Fluorescence: Principles and Applications*, Wiley-VCH Verlag GmbH, Weinheim, 2001.
49 E. P. Serjeant and B. Dempsey, *Ionisation constants of organic acids in aqueous solution*, Pergamon Press, New York, 1979.
50 A. Credi and L. Prodi, Inner filter effects and other traps in quantitative spectrofluorimetric measurements: Origins and methods of correction, *J. Mol. Struct.*, 2014, **1077**, 30–39.